Complexation of arsenite, arsenate, and monothioarsenate with oxygen-containing functional groups of natural organic matter: An XAS study

Biswas, A.; Besold, J.; Sjöstedt, C.; Gustafsson, J. P.; Scheinost, A. C.; Planer-Friedrich, B.;

Originally published:

August 2019

Environmental Science & Technology 53(2019), 10723-10731

DOI: https://doi.org/10.1021/acs.est.9b03020

Complexation of arsenite, arsenate, and monothioarsenate to alcoholic functional groups of natural organic matter: Insights from X-ray absorption spectroscopy

Ashis Biswas[1,2]*, Johannes Besold[1], Carin Sjöstedt[3], Jon Petter Gustafsson[3], Andreas C. Scheinost[4,5], Britta Planer-Friedrich[1]

[1]*Department of Environmental Geochemistry, Bayreuth Center for Ecology and Environmental Research (BAYCEER), Bayreuth University, 95440 Bayreuth, Germany*

[2]*Department of Earth and Environmental Sciences, Indian Institute of Science Education and Research (IISER) Bhopal, Bhopal Bypass Road, Bhauri 462066, Madhya Pradesh, India*

[3]*Department of Soil and Environment, Swedish University of Agricultural Sciences, Box 7014, 750 07, Uppsala, Sweden*

[4]*The Rossendorf Beamline (ROBL) at ESRF, 38043 Grenoble, France*

[5]*Institute of Resource Ecology, Helmholtz-Zentrum Dresden-Rossendorf (HZDR), Bautzner Landstraße 400, 01328 Dresden, Germany*

***Contact and corresponding author: Ashis Biswas (phone: +91 755 269 1389; e-mail:** ashis@iiserb.ac.in**)**

17 **TOC Art**

18

19

ABSTRACT

This study investigated the potentiality of arsenite (~~As(III))~~, arsenate ~~(As(V))~~, and monothioarsenate (MTAs(V)) complexation to alcoholic groups of natural organic matter (NOM). The extent of complexation was highest for As(III), followed by MTAs(V) and As(V). Complexation was higher at pH 7.0 than at pH 4.5 for As(III) and As(V), vice versa for MTAs(V) due to partial transformation to As(III) at pH 4.5. Conditional distribution coefficients were considerably lower than those for complexation through organic thiol groups, but comparable to those for ternary complexation through Fe^{3+} bridging. EXAFS modelling of the As K-edge spectra revealed monodentate and bidentate complexation of the AsO_3 pyramid but tridentate complexation of the AsO_4 and the $AsSO_3$ tetrahedra to alcoholic groups of peat. The higher denticity and an observed longer As-C interatomic distance in As(V)- and MTAs(V)-treated peat - as compared to As(III)-treated peat - is attributed to electrostatic repulsion between negatively charged peat and As species. This study implies that complexation through alcoholic groups of NOM can be an additional or alternative mode of As sorption and depending on acidity of the functional NOM groups, As(V) species can have a higher mobility than arsenite in NOM-rich environments.

Keywords. Arsenic; biogeochemistry; sorption; peat; EXAFS

INTRODUCTION

Over the last four decades, the natural and anthropogenic occurrences of elevated concentrations of arsenic (As) in surface waters, groundwaters, and agricultural soils have been highlighted as a potential environmental concern in many parts of the world.[1–3] It is estimated that only in Southeast Asia more than 100 million of people are at risk of chronic As toxicity from drinking water and food consumption.[4] Therefore, it is necessary to characterize different biogeochemical processes that regulate the mobility of As in the aquatic and terrestrial ecosystems.

Formation and inter-conversion of different As species determine the extent of its mobility in the environment.[1] Two most commonly reported inorganic As species are penta-valent arsenate (As(V)) and tri-valent arsenite (As(III)) which predominate under strongly oxidizing conditions and moderately oxidizing to moderately reducing conditions, respectively.[1] After recent advances in analytical speciation technique, it has become evident that under anoxic sulfidic conditions thiolated penta-valent As species, so-called thioarsenates ($H_xAsS_nO_{4-n}^{3-x}$; n = 1−4; x = 1−3), can also be formed in significant quantities under diverse natural settings.[5–11] Extent of sorption of these As species onto different mineral matters, specially metal oxyhydroxides in soils and sediments is identified as one of the key regulating processes for their mobility in the environment.[1,12–14] Recently, a series of studies have highlighted the potentiality of natural organic matter (NOM) as an alternative or additional sorbent for As and its regulatory role in the As mobilization and transport process in the surface and sub-surface environments.[15–21]

Natural organic matter, being the decomposition product of animal, plant and soil biomass is abundant in aquatic and terrestrial ecosystems.[16] It has a complex structure with a variety of functional groups, such as carboxylic, alcoholic, esteric, quinone, amino, nitroso, thiol, hydroxyl etc., which are mostly negatively charged at near-neutral pH.[16] Several mechanisms for the binding of As(V) and As(III) to NOM have been put forward. One spectroscopically well characterized mechanism is the formation of ternary complexes through polyvalent metal cation (e.g. Fe^{3+}, Al^{3+}, Ca^{2+}, etc.) bridging between negatively charged or neutral As species and negatively charged NOM (As-M-NOM; M represents polyvalent metal cations).[17,22–26] Another mechanism is the binary complexation by direct binding of As species to the specific functional group of NOM. The most prominent site for such binary complexation can be organic thiol groups (–SH).[21,27] Langner et al.[21] by using X-ray absorption spectroscopy (XAS) have found

almost 100% of As(III) to be bound to thiol groups in the deep peat layer of a minerotrophic peat bog (*Gola di Lago*). A follow-up study has shown that As(III) binding by thiol group can be competitive to its binding by ferrihydrite.[28] Recently, Catrouillet et al.[29,30] have developed a geochemical model for As(III) complexation to NOM by thiol group and via Fe^{2+} and Fe^{3+} bridging. Liu and Cai,[31] on the other hand, have reported two types of binding sites (strong and weak sites) to be involved during binary complexation of As(III) with Aldrich Humic Acid (AHA); although, they did not attempt to characterize the binding sites.

Few studies have highlighted that alcoholic (–OH) groups (aliphatic and/or aromatic, specially phenol), a highly abundant functional group in NOM,[32] can also be a potential binding site for binary complexation of As species to NOM. For example, Buschmann et al.[18] in a dialysis experiment found that 26% As(III) and 62% As(V) of total spiked concentrations bound to AHA and estimated that under environmentally relevant conditions at least 10% As(V) should be bound to dissolved organic carbon (DOC) in aquatic environments. They hypothesized that OH^- ligand exchange reaction between As species and alcoholic groups of NOM could be the underlying mechanism of such bindings; although, they did not present any spectroscopic evidence in support of their hypothesis. Lenoble et al.[33] have investigated the interaction of As(III) and As(V) to Suwanee River Humic Acid (SRHA) in the absence and presence of Ca^{2+} by fluorescence spectroscopy. Based on sorption data and fluorescence quenching phenomena of SRHA they concluded the formation of only a binary complex for As(III) and a mixture of binary and Ca^{2+} bridged ternary complexes for As(V). They have determined the stability constant of these complexes assuming monodentate binding to alcoholic group of SRHA, without further effort to characterize the type of functional group involved in the complexation and mode of binding. Evidence of As-O-C bond formation by ligand exchange reaction between alcoholic group of NOM and As species is given by Hoffmann et al.[26] and Guénet et al.[34] During modelling of As K edge EXAFS spectra of the samples obtained by equilibrating As(III) with Fe spiked peat Hoffmann et al.[26] had to include C in addition to Fe for the second shell. They have determined coordination numbers (CN) of 1.5 to 2.0 for C at the distance of 2.70 to 2.77 Å from the As. However, they have mentioned that due to signal contribution from Fe backscatterer at similar distance, the CN of C must be treated with caution. They have further estimated that at least 27% of total As(III) was bound to phenolic groups, in addition to ternary complexation via Fe^{3+} bridging. Similarly, Guénet et al.[34] have provided XAS based evidence for the complexation

of As(V) and As(III) mixtures to alcoholic groups of organic matter, in addition to their bindings to Fe nanoparticle aggregates in the size fraction of 5-0.2 μm during oxidation of reduced soil suspension solution. However, to the best of our knowledge, so far it has never been attempted to investigate the extent of As(III) and As(V) bindings to NOM by complexation exclusively to the alcoholic group, with spectroscopic evidence of As-O-C bond formation. Unavailability of this information obscures the potentiality of As(III) and As(V) bindings to NOM when polyvalent metal cation content in the system is too low for ternary complexation and thiol group content in NOM is not large enough to make significant thiol coordination. It is worth highlighting that the complexation of thioarsenate to alcoholic group of NOM has never been tested at all.

The objective of the present study was to investigate the potentiality and determine the structural parameters for ligand exchange binary complexation of different As species (including thioarsenate) to alcoholic groups of NOM. The objective was accomplished by equilibrating individual As species with low metal containing purified-peat (as a representative for NOM) under anoxic conditions, followed by determining the local coordination environment (up to 4 Å) of As in the peat by As K edge XAS analysis. The findings of this study will help to better constrain the geochemical model for simulating the interaction of As species with NOM in aquatic and terrestrial environments. In general, this study will also develop our limited understanding of neutral to oxyanionic species complexation to NOM, a topic that is not as developed as metal cation complexation to NOM.[18]

MATERIALS AND METHODS

Materials. This study used low metal containing purified-peat as a model NOM compound. Collection, purification, and characterization of this peat are presented in Besold et al.[35] Monothioarsenate (hereafter referred as MTAs(V)) was used as the representative of thioarsenate species, since it is often reported as the major thioarsenic species formed under diverse natural settings and is structurally analogous to the As(V).[6,35–37] Because there is no commercial standard, MTAs(V) was synthesized in the laboratory, with a purity of 90% (5% arsenate and 5% arsenite).[35] All other chemicals of analytical grade, including As(III) and As(V) standards, were purchased from Fluka, Alfa Aesar, or Sigma-Aldrich. All the glasswares used in this study were acid-washed and dried before use.

Sorption experiment. An equilibrium-sorption experiment was conducted for individual As species at pH 4.5 (±0.3) and 7.0 (±0.3). For this experiment, 0.2 g of dry peat was incubated with variable concentrations (0 – 1000 µM) (0 – 4.6 mmol As/mol C) of each As species in an anoxic background electrolytic solution of 30 mM NaCl in glass septum bottles capped and sealed with butyl rubber stoppers and aluminum caps. Incubation was conducted for 96 h in an end over end shaker in the dark under anoxic conditions (pO_2 <1 ppm) at ambient temperature. The duration of 96 h was selected for incubation so that the results can be directly compared to the studies of Hoffmann et al.[26,27] which have used the same peat to investigate As(III) bindings through binary organic thiol coordination and Fe^{3+} bridged ternary complex formation. To avoid microbial activity, 0.15 mM NaN_3 (0.75 mmol/mol C) was added to the reaction medium. The desired pH was adjusted with anoxic HCl and NaOH solution. After equilibration, the peat-solution slurry was filtered through 0.2 µm nylon filter using a vacuum filtration unit inside the glove box. The peat residue was freeze-dried, homogenized, and stored in the dark at ambient temperature inside the glove box until analyses. The amount of As sorbed to peat was determined after microwave-assisted digestion followed by quantification of As by inductively coupled plasma-mass spectrometry (ICP-MS).[35] The conditional distribution coefficient (K_{OC}) (L/kg) of As was determined as: $K_{OC} = C_P/C_S$, where C_P and C_S represent As concentration in peat (µg/kg) and As concentration in solution (µg/L) after equilibration, respectively. C_S was determined by subtracting the amount of As sequestered into peat from the solution.

Arsenic K edge XAS analysis. To determine the local coordination environment of As in the peat after equilibration, As K edge (11867 eV) XAS analysis was performed at the Rossendorf Beamline (ROBL) at the European Synchrotron Radiation Facility (ESRF), Grenoble, France and at the beamline 11-2 of the Stanford Synchrotron Radiation Lightsource (SSRL), Stanford, USA. To aid the modelling of the sample spectra, triethoxyarsine ($(C_2H_5O)_3As$) (TEA) was measured as a reference standard at ROBL, ESRF. Samples were measured in fluorescence mode, while the TEA standard was measured in transmission mode. Samples and the standard were measured at about 15 K using a He cryostat to avoid beam damage and to minimize thermal disorder in the structure. Details on beamline setup, sample preparation, analysis, data reduction, and modelling are provided in the supporting information.

RESULTS AND DISCUSSION

Complexation of As species to peat. Amounts of As sorbed to peat at different equilibrated concentrations of the three As species at pH 4.5 and 7.0 are illustrated in Figure 1. Among the three tested species, maximum sorption was observed for As(III), followed by MTAs(V) and As(V). Earlier studies have reported higher sorption of As(V) to AHA and SRHA compared to As(III);[18,22,38] the possible reason for this inconsistency is discussed in the following section after determination of the binding mechanism. The maximum sorption capacity of the peat was not exhausted even with the highest equilibrated As(III) concentration of 1000 μM (4.6 mmol As/mol C). In agreement with earlier studies,[18,22,31,33,38] the sorption of As(III) and As(V) was higher at pH 7.0. The pH effect was more prominent for As(III) compared to As(V). However, for MTAs(V) the sorption was higher at pH 4.5, which can be attributed to the partial transformation of MTAs(V) to As(III) at this pH, as reflected by the XANES spectra discussed in the following section. The calculated log K_{OC} (L/kg) at pH 7.0 were 0.83 – 1.01 (mean: 0.90) for As(III), 0.40 – 0.56 (mean: 0.47) for MTAs(V), and 0.34 – 0.41 (mean: 0.38) for As(V); at pH 4.5 corresponding values were 0.73 – 0.85 (mean: 0.78), 0.44 – 0.66 (mean: 0.52), and 0.31 – 0.38 (mean: 0.35). With experimental uncertainty, the log K_{OC} decreased with the increase of equilibrated As concentration (more specifically with the increase of equilibrated As/NOM ratio as the amount of NOM was fixed to 0.2 g) in the system for all three As species at both pH (Figure SI-1). Although no explanation is offered, earlier studies have also reported similar decreasing trend of distribution coefficients for As(V) and As(III) binding to NOM with increasing As/NOM ratios.[18,31] Hoffmann et al.[26,27] have determined the log K_{OC} values at pH 7.0 by equilibrating 0.275 mmol As(III)/mol C of the same peat spiked with variable amount of S(-II) and Fe^{3+}. The values for As(III) at pH 7.0 of the present study (0.83 – 1.01) are considerably lower than the values (0 – 2.9) obtained after spiking with S(-II), but comparable to that (1.2 – 1.5) obtained after spiking with Fe^{3+}.

EXAFS modelling and complexation mechanism. Normalized As K edge XANES spectra of peat after equilibration with As(III), As(V), and MTAs(V) at two pH together with various reference standards are displayed in Figure SI-2. The E_0 of peat equilibrated with As(III) and As(V) at both pH appeared at the respective position of As(III) (~11869 eV) and As(V) (~11873 eV) reference standards, indicating no species transformation during equilibration. Similarly, MTAs(V) was not transformed to other species at pH 7.0, indicated by the similar E_0

of the samples and reference standard at ~11871 eV. However, at pH 4.5 the spectra of the two MTAs(V) treated peat samples showed two humps at the position of MTAs(V) and As(III) standards, suggesting partial transformation of MTAs(V) to As(III) during equilibration at this pH. Our earlier study [35] has shown that MTAs(V) can be transformed into As(III) at acidic pH in the presence of S(-II) treated peat, which makes the transformation reaction kinetically feasible by sorbing As(III) (product of transformation) from the solution. The present study suggests that this acid-assisted transformation will be feasible in the presence of any sorbent that sorbs As(III) more strongly than MTAs(V). Based on the findings from XANES spectra, EXAFS modelling was performed for all analyzed peat samples equilibrated with As(III) and As(V) at two pH and MTAs(V) at pH 7.0 only; for the two peat samples equilibrated with MTAs(V) at pH 4.5, linear combination fit (LCF) analysis was performed.

To better constrain sample spectra during EXAFS modelling, the spectrum of TEA was modelled first (Figure SI-3). The major peak at R+ΔR ~1.3 Å in the FT is due to the nearest neighbor O of the AsO_3 pyramid. This major peak was followed by a small FT peak at R+ΔR ~2.2 Å, which can be assigned to C in the second shell.[26,39] Quantitative structural parameters of these two shells were determined by shell-fit analysis. The final model for TEA included As-O and As-C single-scattering (SS) paths and triangular As-O-C multiple-scattering (MS) path. Parameterization (CN: path degeneracy or coordination number, R: interatomic distance or mean half path length (bond length for first shell atom), and σ^2: Debye – Waller parameter) of these paths are presented in Table SI-1. Furthermore, the triangular As-O-O MS path within the AsO_3 pyramid (Table SI-1) was also tested, but finally discarded, since it did not improve the fit significantly. The fitted R and σ^2 of the As-O and As-C paths were 1.78 Å and 0.0021 and 2.78 Å and 0.0059, respectively (Table SI-2), which are consistent with reported values.[26]

The k^3-weighted As K edge EXAFS spectra and their corresponding FT (magnitudes and real parts) of the peat samples equilibrated with As(III) and As(V) at the two pH and MTAs(V) at pH 7.0 are shown in Figure 2. Qualitative Morlet wavelet transforms (WT) analysis of As K edge EXAFS spectra of the samples did not indicate the presence of any heavy backscatterer in the second or higher shell (Figure SI-4). Similar to TEA, FT of the k^3-weighted EXAFS spectra of As(III)-, As(V)-, and MTAs(V)-treated peat samples were characterized by two peaks: a major peak at R+ΔR ~1.3 Å corresponding to nearest neighbor O in the first shell and a small peak at

R+ΔR ~2.2 Å for As(III) (Figure 2A) and ~2.3 Å for As(V) and MTAs(V) (Figure 2B,C) corresponding to C in the second shell. For MTAs(V)-treated peat samples, an additional peak appeared at R+ΔR ~1.8 Å (Figure 2C), which can be attributed to S in the first shell.[36] Accordingly, for all peat samples except #As(V)/4.5/500, inclusion of As-O and As-C SS paths (Table SI-1) in the structural model was essential to fit the sample spectra. For the three MTAs(V)-treated samples, additional As-S SS path (Table SI-1) was also necessary for the fitting. For the sample #As(V)/4.5/500, despite the small FT peak at R+ΔR ~2.3 Å the addition of As-C SS path to the model after As-O SS path and MS paths within the AsO_4 tetrahedra (discussed latter) did not improve the fit significantly according to the F-Test, although it decreased the R-factor. Although, the As-O-C MS path was essential to fit the TEA spectrum, this MS path (constrained similarly as for TEA, Table SI-1) did not improve the fit significantly for any samples according to the set criteria for the MS path. For the As(III)-treated peat samples the triangular As-O-O MS path within the AsO_3 pyramid (Table SI-1) was tested and found to be significant only for the sample #As(III)/7.0/150 by decreasing the redχ^2 by 31% compared to the model with only As-O SS path. However, for all As(V) treated samples, when three MS paths within the AsO_4 tetrahedra, namely, triangular As-O-O, colinear As-O-As-O, and non-colinear As-O-As-O (Table SI-1) were included together in the fit, decreased the redχ^2 on average by 52% (38-69%). Similarly, addition of triangular As-O-O and colinear As-O-As-O MS paths within the $AsSO_3$ tetrahedra (Table SI-1) decreased the redχ^2 in the MTAs(V)-treated samples on average by 30% (23-36%), compared to the model with only As-O and As-S SS paths. Therefore, the final fit model included As-O and As-C SS paths for As(III)-treated samples (additional triangular As-O-O MS path for #As(III)/7.0/150); As-O and As-C (except #As(V)/4.5/500) SS paths and three MS paths within the AsO_4 tetrahedra for As(V)-treated samples, and As-O, As-S, and As-C SS paths and two MS paths within the $AsSO_3$ tetrahedra for MTAs(V)-treated samples. The final fits are displayed in Figure 2 and EXAFS parameters are listed in Table 1.

In the As(III)-treated peat samples the average R_{As-O} was 1.79 ± 0.01 Å (±std. dev.) (range: 1.78 – 1.80 Å), consistent with the reported As-O bond lengths in the AsO_3 pyramid.[39,40] For As-C path, the fitted R_{As-C} was 2.73 ± 0.01 Å (2.73 – 2.74 Å) with CN of 1.7 ± 0.6 (1.0 – 2.4). Despite similar oxidation state of As, the fitted R_{As-C} was relatively longer in TEA (2.78 Å) compared to that in peat, which can be attributed to the liquid state of the TEA standard. The fitted R_{As-C}

values suggest that the AsO_3 pyramids were complexed to peat probably through alcoholic groups (aliphatic and/or aromatic) instead of carboxylic group because, in case of complexation through carboxylic groups, shorter R_{As-C} values (2.58 – 2.68 Å) are expected due to possible hydrogen bonding between the H atom of the As(III) and the carbonyl O of the carboxyl group.[26,39] The fitted R_{As-C} and CN_{As-C} values in peat are consistent with the values (R: 2.70 – 2.77 Å, CN: 1.5 – 2.0) determined by Hoffmann et al.[26] for the Fe-spiked peat equilibrated with As(III) (0.275 mmol As(III)/mol C) at the pH of 7.0, 8.4, and 8.8. They have determined relatively longer R_{As-C} at pH ≥8.4 compared to that at pH 7.0; no such difference was observed in the studied pH range (4.5 to 7.0) of the present study. To determine the exact mode of binding, in the next step we fixed the CN_{As-C} to either 1.0 (Figure SI-5) or 2.0 (Figure SI-6) in the fit model, while keeping the fit strategy for the rest of the parameters unchanged. Results show that for the sample #As(III)/7.0/150 redχ^2 was decreased further when CN_{As-C} was fixed to 1.0 (Table SI-3 vs. Table 1), while for the sample #As(III)/7.0/1000, #As(III)/4.5/1000, and #As(III)/4.5/500, redχ^2 was decreased when CN_{As-C} was fixed to 2.0 (Table SI-4 vs. Table 1). For the sample As(III)/7.0/100, redχ^2 was increased in both cases; however, the increment was more when CN_{As-C} was fixed to 2.0 (Tables-SI-3 and 4 vs. Table 1). Therefore, we conclude that irrespective of pH when equilibrated As(III) concentration is low (≤150 µM; 0.69 mmol As(III)/mol C) each AsO_3 pyramid gets complexed to one alcoholic group of peat (monodentate, Figure 3A); whereas, when equilibrated As(III) concentrations is high (≥500 µM; 2.3 mmol As(III)/mol C) the preferential binding mode is the complexation of each AsO_3 pyramid to two alcoholic groups (bidentate, Figure 3B).

Because of higher oxidation state of As, in the As(V)-treated peat the R_{As-O} was considerably shorter (1.69 ± 0.01 Å, 1.68 – 1.69 Å) compared to the R_{As-O} in the As(III)-treated peat samples. These fitted R_{As-O} values are similar to the reported As-O bond lengths within the AsO_4 tetrahedra.[41] The fitted R_{As-C} and CN_{As-C} were 2.83 ± 0.01 Å (2.82 – 2.84 Å) and 3.2 ± 0.2 (3.0 – 3.4), respectively, comparatively higher than that in the As(III)-treated peat samples. When CN_{As-C} was set to 3.0 in the model (Figure SI-7), redχ^2 was decreased on average by 6% for all the samples (Table SI-5 vs. Table 1), suggesting that each AsO_4 tetrahedra was attached to three alcoholic groups of the peat (Figure 3C). It is worth mentioning that even in the sample #As(V)/4.5/500, although fit improvement because of inclusion of the As-C path in the model was not statistically significant, the fitted R_{As-C} (2.79 Å) and CN_{As-C} (2.3) were comparable to

other samples and redχ^2 was decreased by 5% when CN_{As-C} was set to 3.0 (Table SI-6). Guénet et al.[34] have determined comparable R_{As-C} (2.85-2.86 Å), but relatively smaller CN_{As-C} (1.7 – 2.1) for the mixture of As(V) and As(III) in the 5 – 0.2 µm size fraction during oxidation of the reduced soil suspension. The smaller CN_{As-C} may be result from the presence of As(III) in the system; however, in that case a shorter R_{As-C} is also expected. A more probable alternative explanation is that this can be due to the low As-organic carbon ratio (~0.04 mmol As/mol C) in the solution at the starting of oxidation of the reduced soil suspension. This reason will implicate that similar to As(III), at the low concentration of As(V), each AsO_4 tetrahedra will probably be attached to a lower number (<3.0) of alcoholic groups. Similar to As(III) treatment, there was no effect of change in the equilibrium pH on the fitted EXAFS parameters for the As(V) treatment (Table 1).

In the MTAs(V)-treated peat, the fitted R_{As-O} was 1.72 ± 0.01 Å (1.71 – 1.72 Å), relatively longer than R_{As-O} in As(V)-treated peat but shorter than As(III)-treated peat. The R_{As-S} was determined as 2.10 ± 0.02 Å (2.08 – 2.11 Å), indicating S was double bonded to As.[36] Suess et al.[36] have determined R_{As-O} and R_{As-S} in pure MTAs(V) standard by EXAFS modelling as 1.70 Å and 2.13 Å, respectively. Despite same oxidation state of As, relatively longer R_{As-O} in the $AsSO_3$ tetrahedra compared to that in the AsO_4 tetrahedra in peat can be attributed to the less positive partial charge on the central As atom because of replacement of the double bonded O with double bonded S, which is less electronegative. For As-C path, the fitted R and CN were 2.80 ± 0.02 Å (2.78 – 2.82 Å) and 3.0 ± 0.4 (2.6 – 3.4), respectively, similar to the values obtained for As(V)-treated peat. Again, fixing of CN_{As-C} to 3.0 (Figure SI-8) decreased the redχ^2 on average by 6% for all the samples (Table SI-7 vs Table 1), suggesting each $AsSO_3$ tetrahedra was attached to three alcoholic groups of the peat (Figure 3D). To the best of our knowledge this is the first study that determines the local coordination environment of As when MTAs(V) is complexed to NOM. Since the number of alcoholic group in the peat equilibrated with all three As species was the same, the higher CN_{As-C} in the As(V)- and MTAs(V)-treated peat (CN 3) explains why the extent of sorption of these two As species was less compared to As(III) (CN 1-2) (Figure 1). Furthermore, increase of CN_{As-C} with the increase of equilibrated As concentration (clearly identified for As(III) system) was probably the reason for decreased log K_{OC} with the increase of As/NOM ratio (Figure SI-1). The LCF analysis of the two peat samples equilibrated with MTAs(V) at the pH 4.5 (Figure SI-9) indicated they were a mixture of almost equal

proportion (Table SI-8) of MTAs(V) (44 – 58%) and As(III) (44 – 60%) complexed to peat with the above determined coordination environments.

Above presented modelling of the As K edge EXAFS data of peat equilibrated with different As species has identified two types of complex to be formed for As(III) and one each for As(V) and MTAs(V) (Figure 3), with the following reaction stoichiometry:

$$R\text{-}OH + As(OH)_3 \leftrightarrow R\text{-}O\text{-}As(OH)_2 + H_2O \ (\leq 0.69 \text{ mmol As(III)/mol C})$$

$$2R\text{-}OH + As(OH)_3 \leftrightarrow (R\text{-}O)_2\text{-}As(OH) + 2H_2O \ (\geq 2.3 \text{ mmol As(III)/mol C})$$

$$3R\text{-}OH + HAsO_4^{2-} + 2H^+ \leftrightarrow (R\text{-}O)_3\text{-}AsO + 3H_2O$$

$$3R\text{-}OH + HAsSO_3^{2-} + 2H^+ \leftrightarrow (R\text{-}O)_3\text{-}AsS + 3H_2O$$

The formation of ester of As(III) and As(V) acid with alcohol is well known.[42–44] The underlying mechanism for this esterification is the nucleophilic attack by the alcoholic group to the partially positively charged As atom in the As species.[18] An increase of nucleophilicity of the alcoholic group and a partial positive charge on the As atom increases the rate and thereby extent of complex formation. Since the nucleophilicity of the alcoholic group increases with an increase of pH, it is expected that the extent of complex formation between As species and the alcoholic group will be more at higher pH, which explains the higher sorption of As(III) and As(V) at pH 7.0 compared to 4.5 in the present study (Figure 1). Few earlier studies have reported that complexation of As(III) and As(V) to NOM is optimum around near-neutral pH,[18,22] because at high pH alcoholic group experiences competition with hydroxyl ion from the reaction medium for the nucleophilic attack to the As center. Among the three tested As species, partial positive charge on the central As atom is highest in the As(V), followed by MTAs(V) and As(III); because in As(V) there is an additional O, double bonded to As compared to As(III) and in MTAs(V) this double bonded O is replaced by the less electronegative S. Therefore, considering the partial positive charge on an As atom the expected order of the extent of complexation for the three As species would be As(V) >MTAs(V) >As(III). In agreement with this expected order earlier studies have reported higher sorption of As(V) compared to As(III) to AHA and SRHA.[18,22,38] However, in the present study with peat this order is found to be exactly opposite, which can be potentially explained by the electrostatic repulsion between peat and As species.

Considering the pKa values of the three As species, at the studied pH range (4.5 and 7.0) the predominant species for As(III) should be neutral H_3AsO_3, whereas for As(V) and MTAs(V) it should be negatively charged $H_2AsO_4^-$/$HAsO_4^{2-}$ and $H_2AsSO_3^-$/$HAsSO_3^{2-}$, respectively.[1,45] Possibly, because of higher acidity of the functional groups, the studied peat is more negatively charged than AHA and SRHA at a specific pH. Therefore, compared to AHA and SRHA, when As(V) and MTAs(V) were equilibrated with peat the effect of electrostatic repulsion between more negatively charged peat and negatively charged As species predominated over the effect of higher partial positive charge on the As center in these two species, resulting in lower sorption. On the other hand, since the predominant As (III) species at the studied pH was neutral, the electrostatic repulsion between negatively charged peat and neutral As species would be low, resulting in higher complexation, despite lower partial positive charge on the As center. This electrostatic repulsion can also explain the more prominent pH effect for As(III) complexation compared to As(V) complexation to peat (Figure 1). During change of pH from 4.5 to 7.0 the effect of increased nucleophilicity of the alcoholic group was largely offset by the increased electrostatic repulsion between the negatively charged peat and As(V) species; whereas, for As(III) this offset was small because of involvement of the neutral species in the complexation. Furthermore, this electrostatic repulsion was also probably responsible for the increased $R_{As\text{-}C}$ and $CN_{As\text{-}C}$ in As(V)- and MTAs(V)-treated peat compared to that in As(III)-treated peat (Table 1). It is worth recalling that in the study of Hoffmann et al.[26] the $R_{As\text{-}C}$ in Fe-spiked peat equilibrated with As(III) was longer at pH $\geq$8.4 than at pH 7.0, which can also be due to the formation of predominantly negatively charged $H_2AsO_3^-$ species at these pH, which are close to the pKa1 of H_3AsO_3 (9.2),[1] resulting in increased electrostatic repulsion. Despite electrostatic repulsion, the driving force for complexation of the As species to alcoholic group of NOM has been attributed to the stability gained by donation of the negative charge of the alkoxide ion (R-O^-) to the partially positively charged As atom and/or additional chelation and hydrogen bonding with nearby functional group.[18]

Environmental implication. This study shows that alcoholic groups of NOM can be an alternative or additional binding site for the binary complexation of different As species to NOM. Although the extent of binding is considerably less compared to the binary complexation through organic thiol groups, it is comparable to the binding through Fe^{3+} bridged ternary complex formation. This study implis that NOM can still be a potential sorbent for different As

371 species in systems that are deficient in polyvalent metal cations for ternary complex formation
372 and where organic thiol group content in NOM is not high enough to make significant thiol
373 coordination. Such conditions may prevail in anoxic sulfur deficient ombrotrophic peat bogs, in
374 paddy soils, or aquifer sediments in Bangladesh and West Bengal, India, where the extent of As
375 toxicity to the local inhabitants is most severe. However, similar complexation in the aqueous
376 phase may increase the mobility of As species, but decrease their toxicity by decreasing free ion
377 concentration. This study further implies that the determination of acidity of the functional
378 groups in NOM is essential to assess the mobility of different As species in NOM-rich
379 environments. When the acidity of the functional groups is high, complexation of As(III) is more
380 compared to As(V) and MTAs(V) and vice versa. Therefore, in systems, where NOM is the
381 predominant sorbent for As species, depending on acidity of the functional groups of NOM,
382 As(V) can have a higher mobility than As(III); this is contrasting to the general assumption often
383 made of arsenate being more mobile than arsenite in the environment.[1]

384 **ACKNOWLEDGEMENTS**

385 This research was funded by the Alexander von Humboldt Foundation, Germany, through a
386 postdoctoral scholarship to AB, and DFG project PL302/20 to BPF. AB acknowledges funding
387 from the Indian Institute of Science Education and Research (IISER) Bhopal
388 (INST/EES/2017081) and the Science and Engineering Research Board (SERB), Department of
389 Science and Technology (DST), Govt. of India (ECR/2017/002353) during preparation of the
390 manuscript. Arsenic K-edge XAS analysis was performed at the European Synchrotron
391 Radiation Facility (ESRF), Grenoble, France, and the Stanford Synchrotron Radiation
392 Lightsource (SSRL), a Directorate of SLAC National Accelerator Laboratory and an Office of
393 Science User Facility operated for the US Department of Energy, Office of Science, Office of
394 Basic Energy Sciences under Contract No. DE-AC02-76SF00515. We are also thankful to C.
395 Kerl and D. Halder (University of Bayreuth), A. Rossberg (ESRF), and R. Davis (SSRL) for
396 their support during data collection at the ROBL and 11-2 beamlines.

397 **SUPPORTING INFORMATIONS**

398 Additional tables, figures, and analytical methods.

399 **REFERENCES**

400 (1) Smedley, P. L.; Kinniburgh, D. G. Source and Behaviour of Arsenic in Natural Waters.

401 *Appl. Geochem.* **2002**, *17*, 517–568.
402 (2) Nordstrom, D. K. Of Arsenic in Ground Water. *Science* **2002**, *296*, 64–65.
403 (3) Brammer, H.; Ravenscroft, P. Arsenic in Groundwater: A Threat to Sustainable
404 Agriculture in South and South-East Asia. *Environ. Int.* **2009**, *35* (3), 647–654.
405 (4) Fendorf, S.; Michael, H. A.; Van Geen, A. Spatial and Temporal Variations of
406 Groundwater Arsenic in South and Southeast Asia. *Science* **2010**, *328*, 1123–1127.
407 (5) Stauder, S.; Raue, B.; Sacher, F. Thioarsenates in Sulfidic Waters. *Environ. Sci. Technol.*
408 **2005**, *39* (16), 5933–5939.
409 (6) Planer-Friedrich, B.; London, J.; Mccleskey, R. B.; Nordstrom, D. K.; Wallschläger, D.
410 Thioarsenates in Geothermal Waters of Yellowstone National Park: Determination,
411 Preservation, and Geochemical Importance. *Environ. Sci. Technol.* **2007**, *41* (15), 5245–
412 5251.
413 (7) Wallschläger, D.; Stadey, C. J. Determination of (Oxy)Thioarsenates in Sulfidic Waters.
414 *Anal. Chem.* **2007**, *79* (10), 3873–3880.
415 (8) Planer-Friedrich, B.; Suess, E.; Scheinost, A. C.; Wallschlager, D. Arsenic Speciation in
416 Sulfidic Waters : Reconciling Contradictory Spectroscopic and Chromatographic
417 Evidence. *Anal. Chem.* **2010**, *82*, 10228–10235.
418 (9) Suess, E.; Wallschläger, D.; Planer-Friedrich, B. Stabilization of Thioarsenates in Iron-
419 Rich Waters. *Chemosphere* **2011**, *83* (11), 1524–1531.
420 (10) Stucker, V. K.; Williams, K. H.; Robbins, M. J.; Ranville, J. F. Arsenic Geochemistry in a
421 Biostimulated Aquifer: An Aqueous Speciation Study. *Environ. Toxicol. Chem.* **2013**, *32*
422 (6), 1216–1223.
423 (11) Stucker, V. K.; Silverman, D. R.; Williams, K. H.; Sharp, J. O.; Ranville, J. F. Thioarsenic

Species Associated with Increased Arsenic Release during Biostimulated Subsurface Sulfate Reduction. *Environ. Sci. Technol.* **2014**, *48* (22), 13367–13375.

(12) Dixit, S.; Hering, J. Comparison of Arsenic (V) and Arsenic (III) Sorption onto Iron Oxide Minerals: Implications for Arsenic Mobility. *Environ. Sci. Technol.* **2003**, *37* (18), 4182–4189.

(13) Couture, R. M.; Rose, J.; Kumar, N.; Mitchell, K.; Wallschläger, D.; Van Cappellen, P. Sorption of Arsenite, Arsenate, and Thioarsenates to Iron Oxides and Iron Sulfides: A Kinetic and Spectroscopic Investigation. *Environ. Sci. Technol.* **2013**, *47* (11), 5652–5659.

(14) Biswas, A.; Gustafsson, J. P.; Neidhardt, H.; Halder, D.; Kundu, A. K.; Chatterjee, D.; Berner, Z.; Bhattacharya, P. Role of Competing Ions in the Mobilization Ofarsenic in Groundwater of Bengal Basin: Insight from Surface Complexation Modeling. *Water Res.* **2014**, *55*, 30–39.

(15) Redman, A. D.; Macalady, D.; Ahmann, D. Natural Organic Matter Affects Arsenic Speciation and Sorption onto Hematite. *Environ. Sci. Technol.* **2002**, *36* (13), 2889–2896.

(16) Wang, S.; Mulligan, C. N. Effect of Natural Organic Matter on Arsenic Release from Soils and Sediments into Groundwater. *Environ. Geochem. Health* **2006**, *28* (3), 197–214.

(17) Ritter, K.; Aiken, G. R.; Ranville, J. F.; Bauer, M.; Macalady, D. L. Evidence for the Aquatic Binding of Arsenate by Natural Organic Matter - Suspended Fe(III). *Environ. Sci. Technol.* **2006**, *40* (17), 5380–5387.

(18) Buschmann, J.; Kappeler, A.; Lindauer, U.; Kistler, D.; Berg, M.; Sigg, L. Arsenite and Arsenate Binding to Dissolved Humic Acids: Influence of PH, Type of Humic Acid, and Aluminum. *Environ. Sci. Technol.* **2006**, *40* (19), 6015–6020.

(19) Bauer, M.; Blodau, C. Arsenic Distribution in the Dissolved, Colloidal and Particulate

Size Fraction of Experimental Solutions Rich in Dissolved Organic Matter and Ferric Iron. *Geochim. Cosmochim. Acta* **2009**, *73* (3), 529–542.

(20) Sharma, P.; Rolle, M.; Kocar, B. D.; Fendorf, S.; Kapppler, A. Influence of Natural Organic Matter on As Transport and Retention. *Environ. Sci. Technol.* **2011**, *45* (2), 546–553.

(21) Langner, P.; Mikutta, C.; Kretzschmar, R. Arsenic Sequestration by Organic Sulphur in Peat. *Nat. Geosci.* **2012**, *5* (1), 66–73.

(22) Thanabalasingam, P.; Pickering, W. F. Arsenic Sportion by Humic Acids. *Environ. Pollut. Ser. B, Chem. Phys.* **1986**, *12* (3), 233–246.

(23) Sharma, P.; Ofner, J.; Kappler, A. Formation of Binary and Ternary Colloids and Dissolved Complexes of Organic Matter, Fe and As. *Environ. Sci. Technol.* **2010**, *44*, 4479–4485.

(24) Mikutta, C.; Kretzschmar, R. Spectroscopic Evidence for Ternary Complex Formation between Arsenate and Ferric Iron Complexes of Humic Substances. *Environ. Sci. Technol.* **2011**, *45*, 9550–9557.

(25) Liu, G.; Fernandez, A.; Cai, Y. Complexation of Arsenite with Humic Acid in the Presence of Ferric Iron. *Environ. Sci. Technol.* **2011**, *45*, 3210–3216.

(26) Hoffmann, M.; Mikutta, C.; Kretzschmar, R. Arsenite Binding to Natural Organic Matter: Spectroscopic Evidence for Ligand Exchange and Ternary Complex Formation. *Environ. Sci. Technol.* **2013**, *47* (21), 12165–12173.

(27) Hoffmann, M.; Mikutta, C.; Kretzschmar, R. Bisulfide Reaction with Natural Organic Matter Enhances Arsenite Sorption: Insights from X - Ray Absorption Spectroscopy. *Environ. Sci. Technol.* **2012**, *46*, 11788–11797.

(28) Hoffmann, M.; Mikutta, C.; Kretzschmar, R. Arsenite Binding to Sulfhydryl Groups in the Absence and Presence of Ferrihydrite : A Model Study. *Environ. Sci. Technol.* **2014**, *48*, 3822–3831.

(29) Catrouillet, C.; Davranche, M.; Dia, A.; Bouhnik-Le Coz, M.; Pédrot, M.; Marsac, R.; Gruau, G. Thiol Groups Controls on Arsenite Binding by Organic Matter: New Experimental and Modeling Evidence. *J. Colloid Interface Sci.* **2015**, *460*, 310–320.

(30) Catrouillet, C.; Davranche, M.; Dia, A.; Bouhnik-Le Coz, M.; Demangeat, E.; Gruau, G. Does As(III) Interact with Fe(II), Fe(III) and Organic Matter through Ternary Complexes? *J. Colloid Interface Sci.* **2016**, *470*, 153–161.

(31) Liu, G.; Cai, Y. Complexation of Arsenite with Dissolved Organic Matter: Conditional Distribution Coefficients and Apparent Stability Constants. *Chemosphere* **2010**, *81* (7), 890–896.

(32) Tipping, E.; Hurley, M. . A Unifying Model of Cation Binding by Humic Substances. *Geochim. Cosmochim. Acta* **1992**, *56* (10), 3627–3641.

(33) Lenoble, V.; Dang, D. H.; Loustau Cazalet, M.; Mounier, S.; Pfeifer, H. R.; Garnier, C. Evaluation and Modelling of Dissolved Organic Matter Reactivity toward As^{III} and As^{V} - Implication in Environmental Arsenic Speciation. *Talanta* **2015**, *134*, 530–537.

(34) Guenet, H.; Davranche, M.; Vantelon, D.; Bouhnik-Le Coz, M.; Jarde, E.; Dorcet, V.; Demangeat, E.; Jestin, J. Highlighting the Wide Variability in Arsenic Speciation in Wetlands: A New Insight into the Control of the Behavior of Arsenic. *Geochim. Cosmochim. Acta* **2017**, *203*, 284–302.

(35) Besold, J.; Biswas, A.; Suess, E.; Scheinost, A. C.; Rossberg, A.; Mikutta, C.; Kretzschmar, R.; Gustafsson, J. P.; Planer-Friedrich, B. Monothioarsenate Transformation

493 Kinetics Determining Arsenic Sequestration by Sulfhydryl Groups of Peat. *Environ. Sci.*
494 *Technol.* **2018**, *52*, 7317–7326.
495 (36) Suess, E.; Scheinost, A. C.; Bostick, B. C.; Merkel, B. J.; Wallschlaeger, D.; Planer-
496 Friedrich, B. Discrimination of Thioarsenites and Thioarsenates by X-Ray Absorption
497 Spectroscopy. *Anal. Chem.* **2009**, *81* (20), 8318–8326.
498 (37) Härtig, C.; Planer-Friedrich, B. Thioarsenate Transformation by Filamentous Microbial
499 Mats Thriving in an Alkaline, Sulfidic Hot Spring. *Environ. Sci. Technol.* **2012**, *46* (8),
500 4348–4356.
501 (38) Warwick, P.; Inam, E.; Evans, N. Arsenics Interaction with Humic Acid. *Environ. Chem.*
502 **2005**, *2* (2), 119–124.
503 (39) Kamenar, B.; Bruvo, M.; Butumović, J. Structures Involving Unshared Electron Pair. The
504 Crystal Structures of As(OCOCH3)3 and As2O(OCOCH3)4. *Zeitschrift für Anorg. und*
505 *Allg. Chemie* **1993**, *619* (5), 943–946.
506 (40) Ona-Nguema, G.; Morin, G.; Juillot, F.; Calas, G.; Brown, G. E. EXAFS Analysis of
507 Arsenite Adsorption onto Two-Line Ferrihydrite, Hematite, Goethite, and Lepidocrocite.
508 *Environ. Sci. Technol.* **2005**, *39* (23), 9147–9155.
509 (41) Kitahama, K.; Kiriyama, R.; Baba, Y. Refinement of the Crystal Structure of Scorodite.
510 *Acta Crystallogr. Sect. B* **1975**, *31* (1), 322–324.
511 (42) Lang, W. R.; Mackey, J. F.; Gortner, R. A. Some Esters of Arsenious Acid. *J. Chem. Soc.,*
512 *Trans.* **1908**, *93*, 1364–1372.
513 (43) Brill, T. B.; Campbell, N. C. Arsenites and Antimonites. 11. Vibrational, Nuclear
514 Quadrupole Resonance, and Mass Spectral Properties of Arsenic(II1) and Antimony(II1)
515 Esters and Thioesters'. *Inorg. Chem.* **1973**, *12* (8), 1884–1888.

(44) Tsivgoulis, G. M.; Ioannou, P. V. Esterification Equilibrium Constants of Arsonic and Arsinic Acids. *Monatshefte fur Chemie* **2012**, *143* (12), 1603–1608.

(45) Thilo, E.; Hertzog, K.; Winkler, A. Über Vorgänge Bei Der Bildung Des Arsen(V)-Sulfids Beim Ansäuern von Tetrathioarsenatlösungen. *Zeitschrift für Anorg. und Allg. Chemie* **1970**, *373*, 111–121.

523 **TABLE CAPTIONS**

524 **Table 1:** EXAFS parameters determined by shell-fit analysis of the As K edge EXAFS spectra
525 of the peat equilibrated with different concentrations of As(III) and As(V) at pH 4.5 and 7.0 and
526 MTAs(V) at pH 7.0 only.

527

Table 1: EXAFS parameters determined by shell-fit analysis of the As K edge EXAFS spectra of the peat equilibrated with different concentrations of As(III) and As(V) at pH 4.5 and 7.0 and MTAs(V) at pH 7.0 only.

As species	Sample label	k-range	As-O			As-S			As-C			ΔE_0[a]	R-factor[b]	redχ^2[c]
			CN[d]	R[e] (Å)	σ^{2f} (Å^2)	CN	R (Å)	σ^2 (Å^2)	CN	R (Å)	σ^2 (Å^2)	(eV)	(%)	
	7.0/1000	2.2-13.0	**3.0**[g]	1.80(0[h])	0.0022(3)				1.7(4)	2.74(3)	**0.0059**[i]	0.9(6)	1.5	362
	7.0/150	2.2-9.5	**3.0**	1.78(0)	0.0023(3)				1.0(3)	2.73(4)	**0.0059**	1.6(7)	0.6	60
As(III)	7.0/100	2.2-11.0	**3.0**	1.79(0)	0.0031(3)				1.4(3)	2.73(3)	**0.0059**	1.4(6)	1.0	62
	4.5/1000	2.2-12.0	**3.0**	1.80(0)	0.0010(4)				2.1(5)	2.73(3)	**0.0059**	1.1(7)	1.7	144
	4.5/500	2.2-12.0	**3.0**	1.80(1)	0.0006(4)				2.4(5)	2.74(3)	**0.0059**	1.4(8)	2.2	122
	7.0/1000	2.2-12.5	**4.0**	1.69(0)	0.0016(4)				3.2(10)	2.84(2)	**0.0059**	1.7(8)	1.7	407
	7.0/500	2.2-12.5	**4.0**	1.69(1)	0.0009(5)				3.4(14)	2.82(3)	**0.0059**	1.3(11)	3.4	372
As(V)	7.0/250	2.2-12.0	**4.0**	1.68(1)	0.0011(4)				3.1(11)	2.82(3)	**0.0059**	2.1(9)	2.3	110
	4.5/1000	2.2-12.5	**4.0**	1.69(1)	0.0017(4)				3.0(10)	2.82(4)	**0.0059**	0.9(9)	2.1	315
	4.5/500	2.2-12.0	**4.0**	1.68(1)	0.0006(5)							-0.8(9)	3.2	260
	7.0/1000	2.2-12.5	**3.0**	1.71(0)	0.0034(4)	**1.0**	2.08(1)	0.0042(9)	2.6(5)	2.78(2)	**0.0059**	1.0(6)	0.7	171
MTAs(V)	7.0/150	2.2-10.5	**3.0**	1.72(1)	0.0045(5)	**1.0**	2.10(1)	0.0048(10)	2.9(5)	2.82(2)	**0.0059**	1.6(7)	0.6	60
	7.0/100	2.2-10.0	**3.0**	1.72(1)	0.0031(5)	**1.0**	2.11(1)	0.0027(11)	3.4(7)	2.81(2)	**0.0059**	1.0(9)	0.8	33

[a]Energy-shift parameter, was the same for all paths. [b]R-factor = $\Sigma_i(data_i - fit_i)^2/\Sigma_i data)$. [c]red$\chi^2$ = $(N_{idp}/N_{pts})\Sigma_i((data_i - fit_i)/\varepsilon_i)^2$ $(N_{idp} - N_{var})^{-1}$, where N_{idp}: the number of independent points in the model fit, N_{pts}: the total number of data points, N_{var}: the number of variables in the fit, ε_i: the uncertainty in the i^{th} data point. [d]Coordination number (path degeneracy). [e]Interatomic distance or mean half path length (bond distance for atom in the first-shell). [f]Debye – Waller parameter. [g]Values in bold were fixed in the fit. [h]Values in parenthesis represent uncertainty in the last significant figure of the fitted parameters. [i]This value was determined by fitting the TEA (reference standard) spectrum. Various multiple scattering paths (see text for details) were included in the fit and constrained in terms of three single scattering paths (Table SI-1). Passive amplitude reduction factor (S_0^2) was set to 1.0 for shell-fit analysis of all the samples.

FIGURE CAPTIONS

Figure 1: Sorption of three As species to peat at different equilibrated concentrations at pH 4.5 and 7.0. Symbol and replicate represent average and range of the three replicates.

Figure 2: k^3-Weighted As K edge EXAFS spectra and magnitude and real part of the Fourier transforms (FT) of (A) As(III), (B) As(V), and (C) MTAs(V). Grey lines and red dots represent data and model fit, respectively. Sample labels represent equilibrated pH and As concentration.

Figure 3: Schematic presentation of complexes of the three As species with alcoholic group (for simplicity shown as phenol) of peat identified in the present study: (A) monodentate binding of As(III) at ≤0.69 mmol As(III)/mol C, (B) bidentate binding As(III) at ≥2.3 mmol As(III)/mol, (C) tridentate binding of As(V), and (D) tridentate binding of MTAs(V). Color code of the sphere: purple – As, blue – O, yellow – S, and black – C.

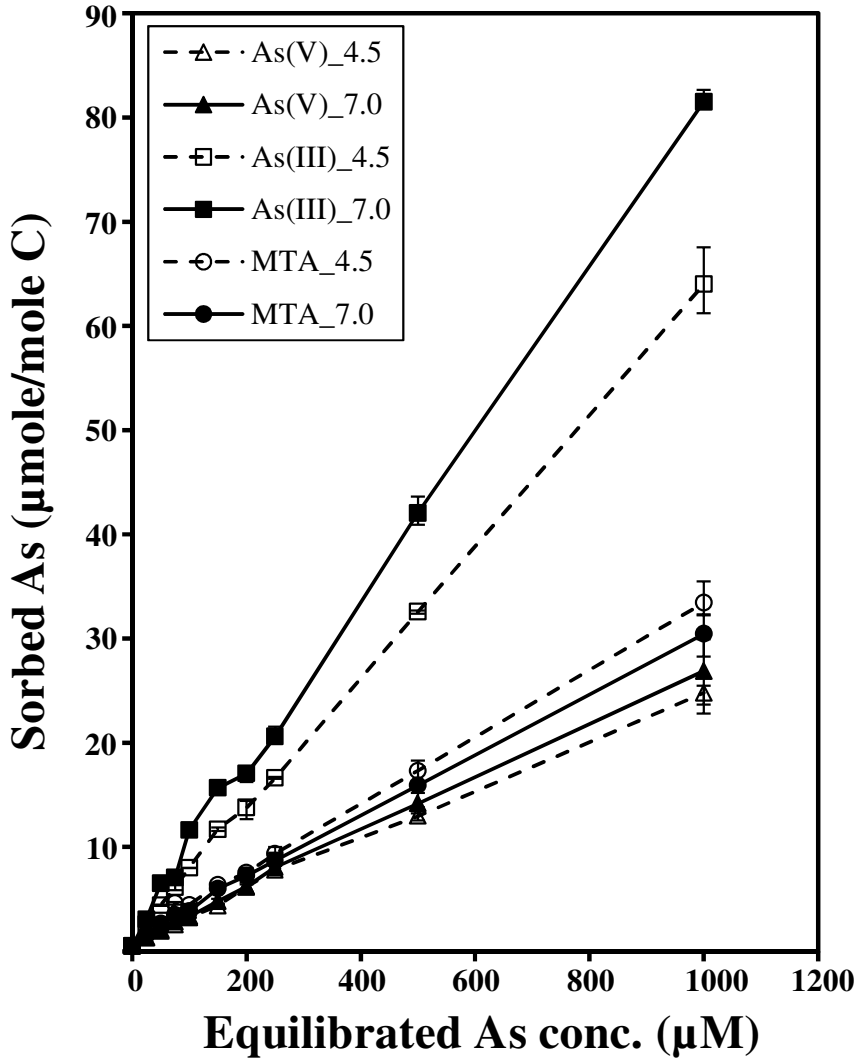

553

554 **Figure 1:** Sorption of three As species to peat at different equilibrated concentrations at pH 4.5

555 and 7.0. Symbol and replicate represent average and range of the three replicates.

556

557

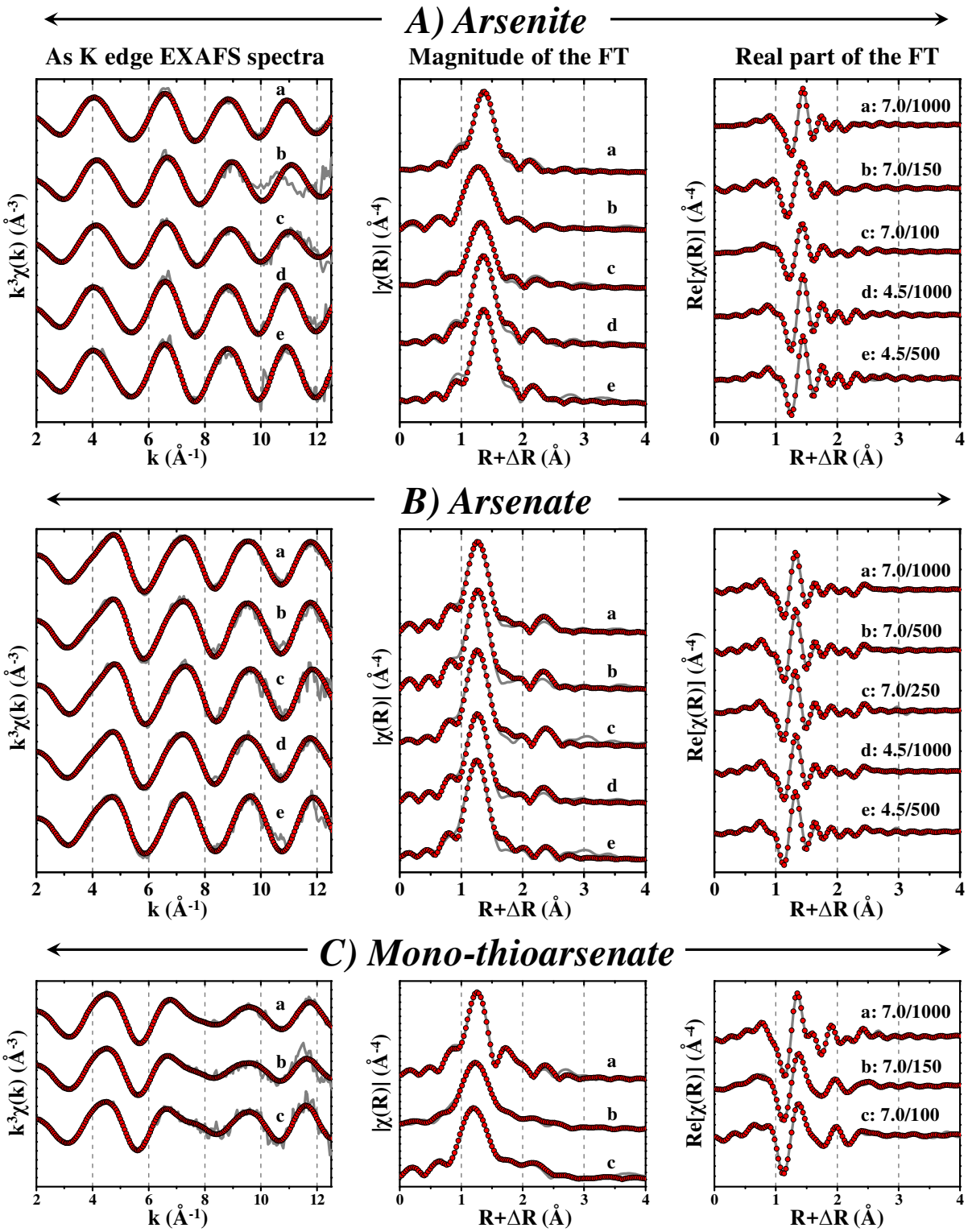

Figure 2: k^3-Weighted As K edge EXAFS spectra and magnitude and real part of the Fourier transforms (FT) of (A) As(III), (B) As(V), and (C) MTAs(V). Grey lines and red dots represent data and model fit, respectively. Sample labels represent equilibrated pH and As concentration.

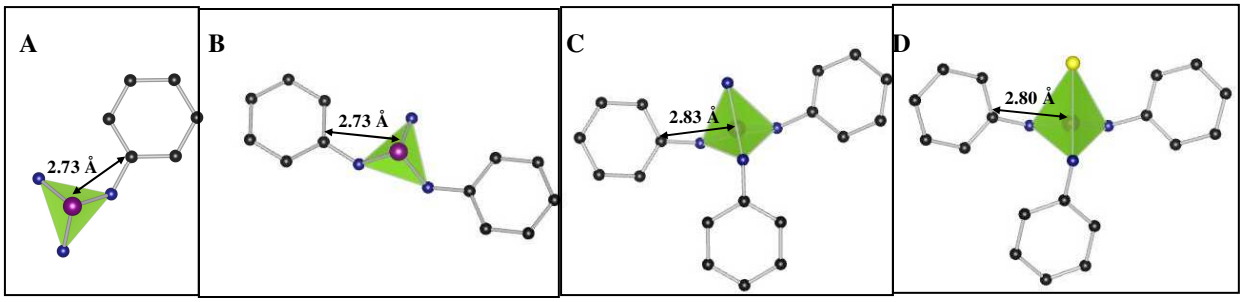

Figure 3: Schematic presentation of complexes of the three As species with alcoholic group (for simplicity shown as phenol) of peat identified in the present study: (A) monodentate binding of As(III) at ≤0.69 mmol As(III)/mol C, (B) bidentate binding As(III) at ≥2.3 mmol As(III)/mol, (C) tridentate binding of As(V), and (D) tridentate binding of MTAs(V). Color code of the spheres: purple – As, blue – O, yellow – S, and black – C.